

Anomalous lattice expansion of coherently strained SrTiO₃ thin films grown on Si(001) by kinetically controlled sequential deposition

J. C. Woicik,¹ H. Li,² P. Zschack,³ E. Karapetrova,³ P. Ryan,⁴ C. R. Ashman,⁵ and C. S. Hellberg⁵

¹National Institute of Standards and Technology, Gaithersburg, Maryland 20899, USA

²Embedded Systems and Physical Sciences Laboratory, Motorola Labs, Tempe, Arizona 85284, USA

³APS-UNICAT, Argonne National Laboratory, University of Illinois, Argonne, Illinois 60439, USA

⁴Ames Laboratory, Ames, Iowa 50011, USA

⁵Center for Computational Materials Science, Naval Research Laboratory, Washington, DC 20375, USA

(Received 27 October 2005; published 25 January 2006)

X-ray diffraction has been used to study the epitaxy and lattice expansion of SrTiO₃ thin films grown coherently on Si(001) by kinetically controlled sequential deposition. The coherent growth of SrTiO₃ on Si produces films with greater in-plane compressive strain than previously attained, -1.66% . The measured expansion of the out-of-plane lattice constant exceeds the prediction of the bulk elastic constants of SrTiO₃ by nearly 100%. This expansion agrees with recent theoretical predictions and experimental findings of room-temperature ferroelectricity in SrTiO₃ films under epitaxial mismatch strain. Our first principles density functional calculations determine an energetically favorable interfacial-defect and surface-charge structure that allows the ferroelectric polarization in these ultrathin films.

DOI: [10.1103/PhysRevB.73.024112](https://doi.org/10.1103/PhysRevB.73.024112)

PACS number(s): 78.70.Ck, 68.55.-a, 68.60.-p

The epitaxial growth of metal oxides on silicon opens the possibility of incorporating many of their unique electronic properties with silicon-device technology. As an example, SrTiO₃ grown commensurately on Si(001) is a strong candidate for ferroelectric memory^{1,2} and ferroelectrically confining quantum dots.³ Additionally, it has recently been shown that the biaxial strain imposed on the perovskite unit cell through hetero-epitaxial growth may be used to engineer both its electronic^{4,5} and structural properties.⁶

Prior report of commensurate SrTiO₃ on Si has been given in the literature,⁷ but there has been no x-ray work presented to support this claim. Although the transmission electron microscopy (TEM) images demonstrate the epitaxial relationship between the cubic perovskite film and the fcc Si substrate: (001)SrTiO₃//(001)Si and SrTiO₃[110]//Si[100], it appears that the interface is not coherent; i.e., it is lacking atom-by-atom registry across the interface. Additionally, the TEM images support an expanded SrTiO₃ in-plane lattice constant that is counter to the in-plane compressive strain that the bulk lattice constants of SrTiO₃ and Si would predict for coherent epitaxial growth.

Here we demonstrate with x-ray diffraction measurements that coherent SrTiO₃ thin films may be grown on Si by a kinetically controlled sequential deposition process (KCSD).⁸ These films have an in-plane lattice constant that is indistinguishable from the Si(001) 1×1 surface-unit cell, and they begin to relax at a critical thickness above ~ 20 Å (5 SrTiO₃ unit cells). They have the greatest in-plane compressive strain reported to date for SrTiO₃ thin-film growth: -1.66% , and they are thin enough to be accessible by first principles calculations.

We find an expanded out-of-plane lattice constant that exceeds the prediction of elastic theory by nearly 100%. This expansion agrees with density functional theory (DFT) calculations of the tetragonal c/a ratio for bulk, ferroelectric SrTiO₃ at this level of in-plane epitaxial strain.⁹ It is also

consistent with Landau-Ginsburg-Devonshire theory of the misfit strain-temperature phase diagram¹⁰ and recent experimental work⁵ that find room-temperature ferroelectricity in epitaxially strained SrTiO₃ thin films, a material that is normally not ferroelectric at any temperature. We present DFT calculations demonstrating that the ferroelectric polarization is allowed through an interfacial-defect and surface-charge structure, supporting recent suggestions that there is no fundamental size limit to ferroelectricity provided that an adequate mechanism exists to screen the electrostatic depolarization field.^{11,12}

All SrTiO₃ films were grown by molecular beam epitaxy (MBE) using an oxide MBE system equipped with Sr and Ti metal effusion cells. High purity molecular oxygen was supplied using a needle valve. A reflective high-energy electron-diffraction (RHEED) system with incident energy of 15 keV and incident angle of 2.5° was used to monitor the growth process *in situ*. Sr to Ti ratio was meticulously calibrated by controlling the characteristic reconstructions of Ti and Sr rich surfaces of SrTiO₃ over an extended deposition period. Other methods similar to those described in Ref. 13 and *in situ* x-ray photoelectron spectroscopy (XPS) analysis were used to confirm that the films had the best possible stoichiometry. The interfaces were found to be atomically sharp and free of SiO₂ using a combination of analyses of TEM, electron-energy loss spectroscopy (EELS), and *in situ* XPS.⁸ Using the KCSD process, two-dimensional growth of SrTiO₃ on Si is achieved by a repetition of depositions that include a low temperature and high oxygen partial pressure (LT-HP) step followed by a high temperature and low oxygen partial pressure (HT-LP) step. This process takes advantage of the fact that oxidation requires both a finite temperature and a sufficient oxygen partial pressure, and the lack of either will suppress the oxidation of the silicon substrate. The deposition of SrTiO₃ began from a Sr template¹⁴ on a clean (free of C and SiO₂) Si surface¹⁵ with substrate temperature at

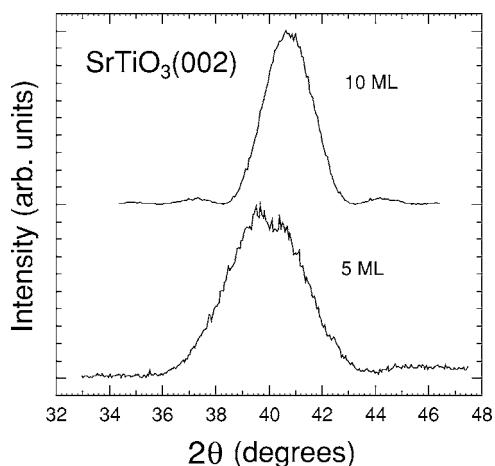


FIG. 1. High-resolution x-ray diffraction $\theta/2\theta$ scans for the 5 ML and 10 ML SrTiO_3 thin films grown on $\text{Si}(001)$. The curves have been scaled to equal peak height.

200 °C–300 °C. Then the LT-HP and HT-LP conditions were alternately applied for every 1–3 monolayers (ML's) of SrTiO_3 growth until the desired thickness was achieved. (Here a ML of SrTiO_3 is defined as a layer of SrTiO_3 with a thickness of one unit cell equal to 3.905 Å.)

X-ray diffraction data were collected at the UNICAT beamline facility 33BM at the Advanced Photon Source using a 4-circle diffractometer and a $\text{Si}(111)$ crystal analyzer. A $\text{Si}(111)$ double-crystal monochromator operating with a pre-collimating mirror and a sagittally bent, horizontally focusing second crystal provided photons with energy 9.0 keV. Figure 1 shows high-resolution $\theta/2\theta$ x-ray diffraction scans from 5 ML and 10 ML SrTiO_3 thin films grown on $\text{Si}(001)$ by KCS. Clearly, the influence of the substrate is evident from the diffraction scans that measure the $\text{SrTiO}_3(002)$ out-of-plane lattice constant. (Cubic SrTiO_3 with a lattice constant of 3.905 Å would appear at a 2θ value of 41.318° on this graph.) Analysis of these data finds the out-of-plane lattice constant for the 5 ML and 10 ML films to be 4.031 ± 0.01 Å and 3.961 ± 0.005 Å, respectively. These lattice constants are significantly larger than the lattice constant of bulk SrTiO_3 , suggesting that these films are under considerable in-plane compressive strain.

To determine the in-plane registry of the SrTiO_3 films relative to the underlying Si lattice, we examined the position of the $\text{SrTiO}_3(200)$ in-plane diffraction relative to the position of the $\text{Si}(220)$ in-plane diffraction. Due to the epitaxial matching condition: $(001)\text{SrTiO}_3 // (001)\text{Si}$ and $\text{SrTiO}_3[110] // \text{Si}[100]$, the SrTiO_3 unit cell is rotated around the $\text{Si}[001]$ direction by 45° , and the position of the $\text{SrTiO}_3(200)$ diffraction for a perfectly coherent epitaxial film would therefore reside at the exact in-plane position as the $\text{Si}(220)$ diffraction. As the $\text{Si}(001)$ 1×1 surface-unit-cell length is $a_{\text{Si}}/\sqrt{2} = 5.43095 \text{ Å} / \sqrt{2} = 3.840 \text{ Å}$ and the SrTiO_3 lattice constant is 3.905 Å, coherent epitaxy results in a compressive mismatch strain between the SrTiO_3 film and the Si substrate that is equal to -1.66% . It is therefore possible to isolate the contribution of the SrTiO_3 layer from the Si substrate by examining the position of the SrTiO_3 in-plane dif-

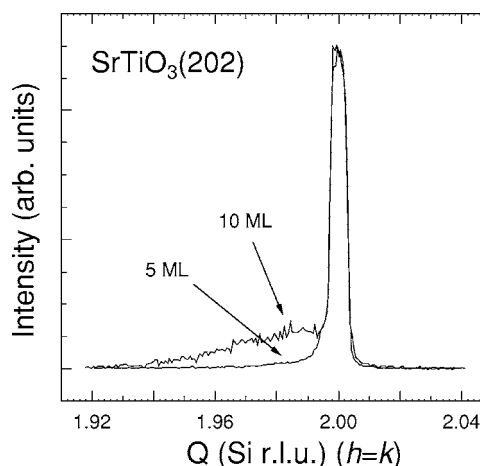


FIG. 2. $h=k$ scans along the $\text{Si}[110]$ direction for the 5 ML and 10 ML films. The curves have been recorded at $l \sim 2.7$ Si r.l.u. (see text) to isolate the SrTiO_3 diffraction from the Si substrate. The curves have been scaled to equal peak height.

fraction, but at an out-of-plane l value that is unique to the out-of-plane lattice constant of the SrTiO_3 film. From the $\theta/2\theta$ scans of Fig. 1, the $\text{SrTiO}_3(002)$ diffraction occurs at a l value of ~ 2.7 in Si reciprocal-lattice units (Si r.l.u.). Therefore, for a perfectly coherent epitaxial film the $\text{SrTiO}_3(202)$ reflection should occur at an (hkl) value of (222.7) in Si r.l.u.

Figure 2 shows $h=k$ scans across the $\text{SrTiO}_3(202)$ Bragg peak for both the 5 ML and 10 ML SrTiO_3 films. These scans were recorded at the l values determined from the $\text{SrTiO}_3(002)$ diffractions for each film (Fig. 1). These curves (as well as pure transverse scans) show sharp, intense peaks at $Q_x = Q_y = 2$ Si r.l.u., demonstrating coherent registry with the Si substrate. For the 10 ML film, however, the intensity of the main peak is ~ 4 times less intense than for the 5 ML film (it has been scaled by a factor of 3.6 in the figure), and there is a second, much broader peak at smaller in-plane momentum transfer. This broad peak is symmetric in both the h and k directions, indicating that the SrTiO_3 deposition past ~ 5 ML's induces the relaxation of the film, while the first 1–2 ML's maintain their registry with the Si substrate. Note, however, that the relaxation of the outermost layers is not complete, for a layer with the bulk, cubic SrTiO_3 lattice constant would peak at $Q_x = Q_y = 1.967$ Si r.l.u. on this curve.

We also examined the transverse scattering around the $\text{SrTiO}_3(002)$ Bragg peak for both the 5 ML and 10 ML films. Figure 3 shows the distribution of scattering around the $\text{SrTiO}_3(002)$ diffraction for the 5 ML film. Two satellite structures appear symmetrically in both h and k with an in-plane momentum transfer that corresponds to an in-plane period of approximately 1200 Å. We attribute these features to the strain fields arising from steps on the $\text{Si}(001)$ surface that are observed in TEM images.⁸ The presence of these satellites confirms that the SrTiO_3 wets the Si surface, producing high quality two-dimensional growth prior to three-dimensional nucleation. (The satellites are barely visible for the 10 ML film.)

Figure 4 shows the measured c/a ratios for the 5 ML and

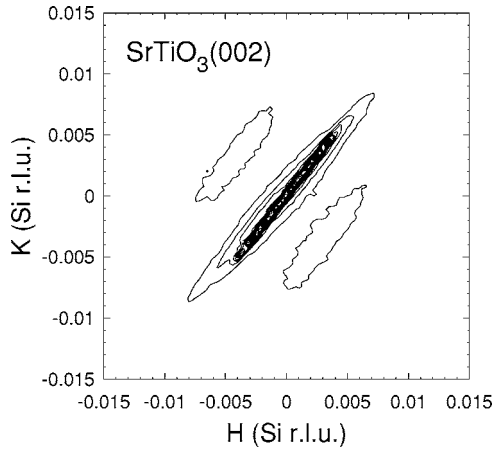


FIG. 3. In-plane distribution of scattering around the $\text{SrTiO}_3(002)$ Bragg peak for the 5 ML film recorded at $l \sim 2.7$ Si r.l.u. The elongation of the features along the $h=k$ direction is due to experimental resolution.

10 ML films as a function of in-plane compressive strain. The in-plane lattice constant for the 5 ML film is equal to the lattice constant of the Si substrate, and the in-plane lattice constant for the 10 ML film is taken from the broad contribution to its $h=k$ curve (Fig. 2). Clearly, the c/a ratios determined by our experiment are much larger than the values predicted by the elastic constants of bulk SrTiO_3 .¹⁶ In fact, the experimentally determined expansion of the perpendicular lattice constant exceeds the prediction of elastic theory by nearly 100%. This expansion agrees with recent theoretical calculations of the c/a ratio of bulk, *ferroelectric* SrTiO_3 with this level of in-plane, compressive biaxial strain.⁹ These calculations find a transformation from a paraelectric tetragonal phase to a noncentrosymmetric ferroelectric phase for films with in-plane compressive strain greater than -0.75% . The c/a ratio is sensitive to the macroscopic polarization due to the strong coupling between polarization and strain.¹⁷ For this reason, x-ray diffraction has been used to identify the onset of ferroelectricity in films that are too thin to be char-

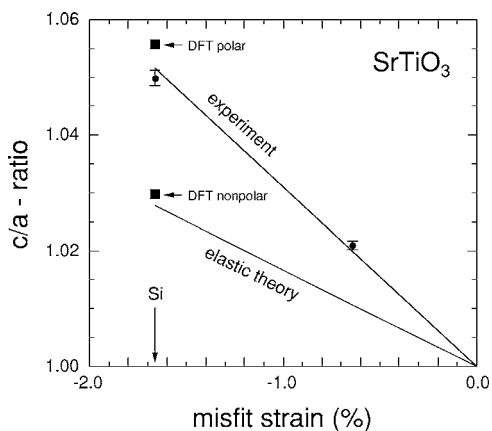


FIG. 4. Measured c/a ratio for the 5 ML and 10 ML films as a function of in-plane lattice mismatch. Also shown are the predictions of elastic theory and the results of our density-functional theory (DFT) calculations.

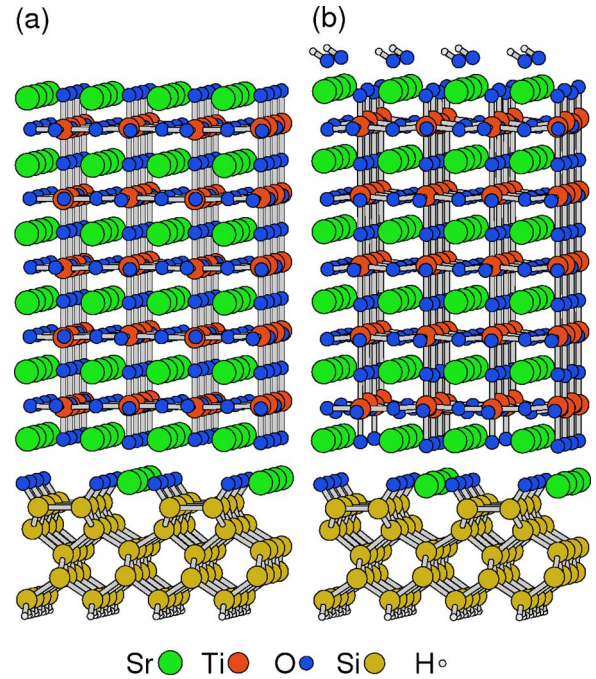


FIG. 5. (Color online) Structure of the ideal 5 ML $\text{SrTiO}_3/\text{Si}(001)$ system (a) and the system with O vacancies near the interface and OH adsorbates on the surface (b). The larger c/a ratio and the polarization of the TiO_2 layers in (b) are readily apparent.

acterized by conventional electrical methods.^{4,11}

It is well known that a polarization in a thin film oriented normal to the surface generates a depolarizing electric field, which, if not screened, will push the ions to an unpolarized state.^{4,11,12,18} The calculations discussed above were performed for infinite, bulk SrTiO_3 films with “short-circuit” periodic boundary conditions.⁹ In order to understand the screening mechanism that allows the polarization within the ultrathin films studied here, we performed first-principles density functional calculations of the entire $\text{SrTiO}_3/\text{Si}(001)$ system using the generalized-gradient approximation (GGA) (Ref. 19) and projector-augmented wave functions as implemented in VASP.²⁰ All calculations were performed on slabs with five layers of Si and five layers of SrTiO_3 ; the Si dimers are bonded to oxygen at the interface and passivated with $1/2$ ML of Sr.^{21,22} A 2×2 supercell was used, which accommodates both the 2×1 structure of the dimerized Si surface and the $\sqrt{2} \times \sqrt{2}$ structure of the rotated oxygen octahedra in SrTiO_3 that occurs under compressive strain.^{10,23} The resulting $\text{SrTiO}_3/\text{Si}(001)$ structure is shown in Fig. 5(a). This structure is the most stable structure found by first principles calculations;²¹ consequently, it is the ideal structure by which to study the possible polarization mechanisms for the $\text{SrTiO}_3/\text{Si}(001)$ interface.

We find that the optimal calculated structure of the ideal system [Fig. 5(a)] with no defects or adsorbates has a c/a ratio of 1.0298, which is much smaller than the experimentally observed c/a ratio and close to the value predicted by elastic theory.^{16,24} This ideal structure has nothing to screen a ferroelectric polarization and indeed we find that it is unpolarized. As the experimental films are likely to contain de-

fects (primarily oxygen vacancies),²⁵ and XPS measurements of these and other films that have been exposed to air find strongly bound OH adsorbates on the surface,²⁶ we also include oxygen vacancies and both H₂O and OH adsorbates in our calculations. Positive O vacancies near the interface and negative adsorbates on the surface are likely candidates to provide the screening required to allow the SrTiO₃ film to polarize, resulting in the large c/a ratio observed by experiment.

We used concentrations of 2(OH) and 1(H₂O) adsorbates per 2×2 surface supercell. Each configuration has two H atoms, so only the O chemical potential is required to determine which configuration is favored. We use the GGA energy of an isolated spin-1 O₂ molecule to determine the O chemical potential. We find H₂O adsorbates are energetically favored over OH adsorbates on the ideal system, and this optimized structure has a c/a ratio of 1.0339, which is also much smaller than the experimentally observed c/a ratio.

To introduce the most likely O vacancies, we calculated the formation energy of a variety of vacancy sites. We find that the vacancies occur most readily directly above the Si dimer row in the SrO layer [see Fig. 5(b)]. This site is favored by 470 meV over a vacancy in the O bonded to the Si, and all other O vacancy sites have even higher energy. We therefore only consider vacancies in the SrO layer above the Si dimer row in our calculations, but we expect that the electrostatic screening will be similar for any O vacancy close to the interface.

With only O vacancies and no adsorbates, we find a c/a ratio of 1.0320. However, with both O vacancies and adsorbates, the situation is quite different. We find OH adsorbates are energetically favored over H₂O adsorbates, the film polarizes to a c/a ratio of 1.0558, and this enhanced c/a ratio is in agreement with the experimentally determined c/a ratio for the coherently strained film.²⁷ This structure is shown in Fig. 5(b). The O vacancies at the interface assume a positive charge while the OH adsorbates on the surface become nega-

tive. Clearly, it is the combination of both vacancies and adsorbates that provides the required screening to compensate the electrostatic depolarization field and allow the system to polarize and expand by the observed amount in the z direction.

The calculated c/a ratios of the nonpolar and polar structures (with and without O vacancies and OH adsorbates) are plotted in Fig. 4. These calculations demonstrate that ferroelectricity can exist in these ultrathin films provided that a mechanism exists by which the depolarization field can be screened. This finding is consistent with recent discovery of nanoscale striped domains in thin ferroelectric films grown on insulating substrates without adsorbates.^{11,12} In the absence of such a screening mechanism, compressively strained ferroelectric films “self-compensate” by forming domains with alternating normal polarization directions.

In conclusion, we have demonstrated that a room temperature ferroelectric polarization in SrTiO₃ thin films grown commensurately on Si(001) by KCSD results from an approximate −1.66% compressive strain as determined by x-ray diffraction measurements. Our results are consistent with both recent theoretical predictions and experimental findings of ferroelectric polarization close to room temperature for strained SrTiO₃ films.^{5,10} The presence of O vacancies and OH adsorbates is the likely source of screening of the ferroelectric depolarization field: without the combination of O vacancies near the interface and OH adsorbates on the surface, the first principles calculations show that films are not able to polarize and do not exhibit the large c/a ratios observed by experiment.

The Advanced Photon Source is supported by the U.S. Department of Energy, Basic Energy Sciences, Office of Science under Contract No. W-31-109-ENG-38. Two of the authors (C.R.A and C.S.H.) acknowledge support from the DARPA QuIST (MIPR 02 N699-00) program. Computations were performed at the ASC DoD Major Shared Resource Center.

¹O. Auciello, J. F. Scott, and R. Ramesh, *Phys. Today* **51**, 22 (1998).

²J. F. Scott, *Ferroelectric Memories* (Springer-Verlag, Berlin, 2000).

³J. Levy, *Phys. Rev. A* **64**, 052306 (2001).

⁴K. J. Choi, M. Bieganski, Y. L. Li, A. Sharan, J. Schubert, R. Uecker, P. Reiche, Y. B. Chen, X. Q. Pan, V. Gopalan, L.-Q. Chen, D. G. Schlom, and C. B. Eom, *Science* **306**, 1005 (2004).

⁵J. H. Haeni, P. Irvin, W. Chang, R. Uecker, P. Reiche, Y. L. Li, S. Choudhury, W. Tian, M. E. Hawley, B. Craigo, A. K. Tagantsev, X. Q. Pan, S. K. Streiffner, L. Q. Chen, S. W. Kirchoefer, J. Levy, and D. G. Schlom, *Nature (London)* **430**, 758 (2004).

⁶F. He, B. O. Wells, and S. M. Shapiro, *Phys. Rev. Lett.* **94**, 176101 (2005).

⁷R. A. McKee, F. J. Walker, and M. F. Chisholm, *Phys. Rev. Lett.* **81**, 3014 (1998).

⁸H. Li, X. Hu, Y. Wei, Z. Yu, X. Zhang, R. Droopad, A. A. Demkov, J. Edwards, K. Moore, W. Ooms, J. Kulik, and P.

Fejes, *J. Appl. Phys.* **93**, 4521 (2003); X. Hu, H. Li, Y. Liang, Y. Wei, Z. Yu, D. Marshall, J. Edwards, Jr., R. Droopad, X. Zhang, A. A. Demkov, and K. Moore, *Appl. Phys. Lett.* **82**, 203 (2003).

⁹A. Antons, J. B. Neaton, K. M. Rabe, and D. Vanderbilt, *Phys. Rev. B* **71**, 024102 (2005).

¹⁰N. A. Pertsev, A. K. Tagantsev, and N. Setter, *Phys. Rev. B* **61**, R825 (2000).

¹¹D. D. Fong, G. B. Stephenson, S. K. Streiffner, J. A. Eastman, O. Auciello, P. H. Fuoss, and C. Thompson, *Science* **304**, 1650 (2004).

¹²N. A. Spaldin, *Science* **304**, 1606 (2004).

¹³J. H. Haeni, C. D. Theis, and D. G. Schlom, *J. Electroceram.* **4**, 385 (2000).

¹⁴Z. Yu, J. Ramdani, J. A. Curless, J. M. Finder, C. D. Overgaard, R. Droopad, K. W. Eisenbeiser, J. A. Hallmark, W. J. Ooms, J. R. Conner, and V. S. Kaushik, *J. Vac. Sci. Technol. B* **18**, 1653 (2000).

¹⁵Y. Wei, X. Hu, Y. Liang, D. C. Jordan, B. Craigo, R. Droopad,

- Z. Yu, A. Demkov, J. John, L. Edwards, and W. J. Ooms, *J. Vac. Sci. Technol. B* **20**, 1402 (2002).
- ¹⁶R. O. Bell and G. Rupprecht, *Phys. Rev.* **129**, 90 (1963).
- ¹⁷R. E. Cohen, *Nature (London)* **358**, 136 (1992).
- ¹⁸P. Ghosez and K. M. Rabe, *Appl. Phys. Lett.* **76**, 2767 (2000); B. Meyer and D. Vanderbilt, *Phys. Rev. B* **63**, 205426 (2001); J. Junquera and P. Ghosez, *Nature (London)* **422**, 506 (2003); M. Dawber *et al.*, *J. Phys.: Condens. Matter* **15**, L393 (2003); C. H. Ahn, K. M. Rabe, and J.-M. Triscone, *Science* **303**, 488 (2004).
- ¹⁹J. P. Perdew, K. Burke, and M. Ernzerhof, *Phys. Rev. Lett.* **77**, 3865 (1996).
- ²⁰G. Kresse and J. Furthmüller, *Phys. Rev. B* **54**, 11169 (1996); G. Kresse and D. Joubert, *Phys. Rev. B* **59**, 1758 (*ibid.* **50**, 17953 (1994)).
- ²¹C. J. Först, C. R. Ashman, K. Schwarz, and P. E. Blöchl, *Nature (London)* **427**, 53 (2004).
- ²²P. W. Peacock and J. Robertson, *Appl. Phys. Lett.* **83**, 5497 (2003).
- ²³The calculations used a 300 eV plane wave cutoff, 8×8 Monkhorst-Pack sampling of the Brillouin zone per 1×1 unit cell, and a vacuum region of 8 \AA between repeated slabs. All structures were relaxed without symmetry constraints. The forces were converged to less than 16 meV/\AA . The hydrogen-terminated lowest Si layer was kept fixed.
- ²⁴Since x rays scatter strongest from the Sr ions, the calculated c/a ratio was determined from the difference in the average heights of the Sr ions in the lowest and highest SrO layers.
- ²⁵D. A. Muller, N. Nakagawa, A. Ohtomo, J. L. Grazul, and H. Y. Hwang, *Nature (London)* **430**, 657 (2004).
- ²⁶S. A. Chambers, Y. Liang, Z. Yu, R. Droopad, J. Ramdani, and K. Eisenbeiser, *Appl. Phys. Lett.* **77**, 1662 (2000).
- ²⁷The calculations were performed at the GGA lattice constant of Si. GGA slightly overestimates the lattice constants of most materials, including SrTiO_3 and Si, but not by the same amount. The GGA lattice constant of Si is 2.03% smaller than SrTiO_3 , so the calculated films are under more compressive strain than the experimental films, which is likely the source of the greater c/a ratios of the DFT systems over the experiment and elastic theory as seen in Fig. 3.